Radiosynthesis and Preclinical Evaluation of ^{11}C-ABP688 as a Probe for Imaging the Metabotropic Glutamate Receptor Subtype 5

Simon M. Ametamey, PhD[1]; Lea J. Kessler, PhD[1]; Michael Honer, PhD[1]; Matthias T. Wyss, MD[2]; Alfred Buck, MD[2]; Samuel Hintermann, PhD[3]; Yves P. Auberson, PhD[3]; Fabrizio Gasparini, PhD[3]; and Pius A. Schubiger, PhD[1]

[1]Center for Radiopharmaceutical Science of ETH, PSI and USZ and Department of Chemistry and Applied Biosciences of ETH, Zurich, Switzerland; [2]PET Center, Division of Nuclear Medicine, University of Zurich, Zurich, Switzerland; and [3]Novartis Institutes for Biomedical Research Basel, Novartis Pharma AG, Basel, Switzerland

^{11}C-ABP688 (3-(6-methyl-pyridin-2-ylethynyl)-cyclohex-2-enone-*O*-^{11}C-methyl-oxime), a noncompetitive and highly selective antagonist for the metabotropic glutamate receptor subtype 5 (mGluR5), was evaluated for its potential as a PET agent. **Methods:** ABP688 was radiolabeled with ^{11}C by reacting ^{11}C-methyl iodide with the sodium salt of desmethyl-ABP688 (3-(6-methyl-pyridin-2-ylethynyl)-cyclohex-2-enone oxime). The affinity of ^{11}C-ABP688 for mGluR5 was determined by Scatchard analysis using rat whole-brain membranes (without cerebellum). Ex vivo autoradiography, biodistribution, and PET studies with ^{11}C-ABP688 were performed on rats, wild-type mice, and mGluR5-knock-out mice. **Results:** The overall synthesis time was 45−50 min from the end of radionuclide production. ^{11}C-ABP688 was obtained in good radiochemical yield (35% ± 8%, n = 17, decay corrected), and the specific radioactivity was 150 ± 50 GBq/μmol (n = 17) at the end of the synthesis. Scatchard analysis revealed a single high-affinity binding site with a dissociation constant of 1.7 ± 0.2 nmol/L and a maximum number of binding sites of 231 ± 18 fmol/mg of protein. Ex vivo autoradiography in wild-type mice and rats showed a heterogeneous distribution pattern consistent with the known distribution of mGluR5 in the brain, with the highest uptake in hippocampus, striatum, and cortex. Blocking studies by coinjection of ^{11}C-ABP688 and unlabeled 2-methyl-6-(3-methoxyphenyl)ethynyl-pyridine (1 mg/kg), an antagonist for mGluR5, revealed up to 80% specific binding in rat brain. In mGluR5-knock-out mouse brain, a homogeneous and markedly reduced accumulation of ^{11}C-ABP688 was observed. PET studies on rats and mice using a small-animal PET scanner also demonstrated radioactivity uptake in the brain regions known to be rich in mGluR5. In contrast, radioactivity uptake in mGluR5-knock-out mice was fairly uniform, substantiating the specificity of ^{11}C-ABP688 binding to mGluR5. **Conclusion:** ^{11}C-ABP688 is a selective tracer for imaging mGluR5 in vivo in rodents and may offer a future tool for imaging mGluR5 in humans using PET.

Received Sep. 19, 2005; revision accepted Dec. 21, 2005.

For correspondence or reprints contact: Simon M. Ametamey, PhD, Center for Radiopharmaceutical Science of ETH, PSI and USZ, ETH-Hönggerberg, D-CHAB IPW HCI H427, Wolfgang-Pauli-Strasse 10, CH-8093 Zurich, Switzerland.

E-mail: simon.ametamey@pharma.ethz.ch

Key Words: metabotropic glutamate receptor subtype 5; ^{11}C-ABP688; mGluR5-knock-out mice; biodistribution

J Nucl Med 2006; 47:698–705

Metabotropic glutamate receptors (mGluRs) are G-protein–coupled receptors. In the central nervous system, mGluRs modulate glutamatergic neurotransmission and are recognized potential therapeutic targets (*1,2*). To date, 8 mGluR subtypes have been identified and classified into 3 groups on the basis of their sequence identity, pharmacology, and preferred signal transduction mechanism. Group 1 mGluRs (mGluR1 and mGluR5) are coupled to phospholipase C and upregulate or downregulate neuronal excitability (*3*). Group 2 (mGluR2 and mGluR3) and group 3 (mGluR4 and mGluR6–8) inhibit adenylate cyclase and hence reduce synaptic transmission.

Excessive activation of mGluR5 has been implicated in a variety of disease states (*2*) such as anxiety (*4,5*), depression (*5*), schizophrenia (*6*), Parkinson's disease (*7*), and drug addiction or withdrawal (*8*). Involvement of mGluR5 in the modulation of various pain states such as acute, persistent chronic, inflammatory, and neuropathic has also been reported (*9–11*).

Noninvasive techniques such as PET or SPECT offer the possibility to visualize and to study mGluR5 under physiologic and pathologic conditions. Although mGluR5 antagonists have been successfully used in vitro to label mGluR5 (*12,13*), their in vivo visualization has been hampered by a lack of selective PET or SPECT ligands. Using the prototypic antagonist MPEP (2-methyl-6-(phenylethynyl)-pyridine) as a template (*14*), we synthesized and evaluated 4 derivatives, namely ^{11}C-2-methyl-6-(3-methoxyphenyl)ethynyl-pyridine (M-MPEP), ^{11}C-2-methyl-6-(3-fluorophenylethynyl)-pyridine (M-FPEP), ^{18}F-2-methyl-6-(3-fluoroethylphenyl)ethynyl-pyridine (FE-MPEP), and ^{18}F-2-fluoro-6-(3-fluorophenylethynyl)-pyridine (FPEP) (Fig. 1), but none of these ligands proved to be useful (*15,16*), possibly because of high lipophilicity, unfavorable brain uptake kinetics, or a

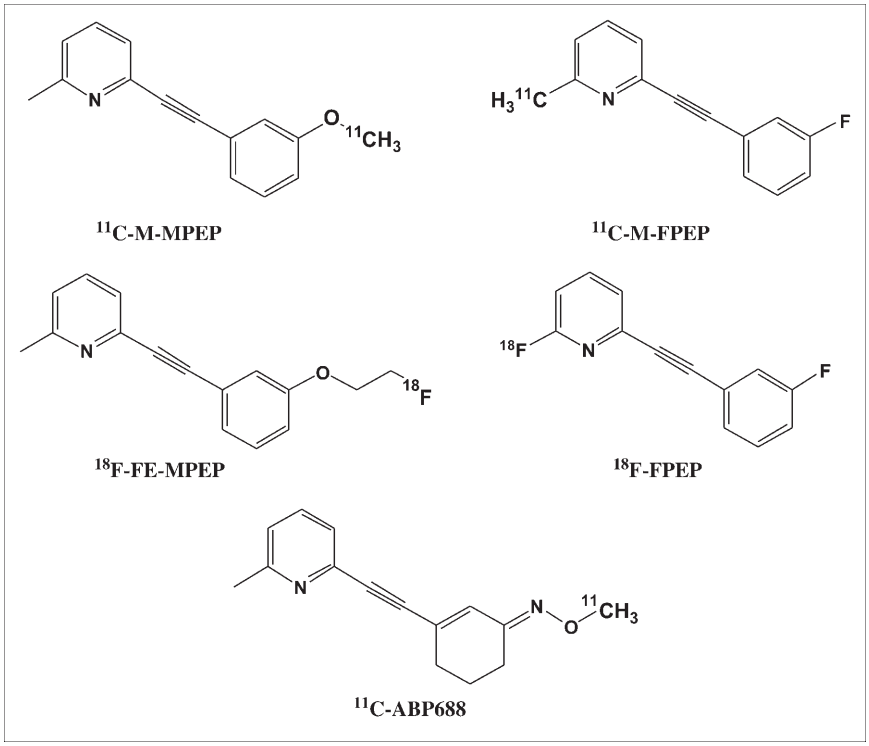

FIGURE 1. Structures of ^{11}C-M-MPEP, ^{11}C-M-FPEP, ^{18}F-FE-MPEP, ^{18}F-FPEP, and ^{11}C-ABP688.

high metabolism. Recently, Hamill et al. (*17*) reported on the successful imaging of mGluR5 in a rhesus monkey brain. While awaiting further evaluation of these ligands, we pursued our efforts to overcome the shortcomings of our previously reported compounds—shortcomings that could be related to the MPEP core—and evaluated ^{11}C-ABP688 (3-(6-methyl-pyridin-2-ylethynyl)-cyclohex-2-enone-*O*-^{11}C-methyl-oxime; Fig. 1). Herein, we describe the radiosynthesis and the preclinical evaluation of ^{11}C-ABP688, a novel, high-affinity, and selective mGluR5 antagonist, as a promising PET tracer.

MATERIALS AND METHODS

Desmethyl-ABP688 was synthesized as described by Kessler (*18*), and its structure was confirmed by nuclear magnetic resonance (^{1}H-NMR) and mass spectroscopy. All other chemicals and solvents were of analytic grade and were used without purification. ^{11}C-Methyl iodide was produced with a PET trace system (GE Healthcare) at the University Hospital in Zurich from ^{11}C-CO_2 in a 2-step reaction sequence involving the catalytic reduction of ^{11}C-CO_2 to ^{11}C-methane and subsequent gas phase iodination according to the standard procedure (*19*).

Radiosynthesis of ^{11}C-ABP688

ABP688 was labeled with ^{11}C by reacting the sodium salt of desmethyl-ABP688 in anhydrous dimethylformamide with ^{11}C-methyl iodide at 90°C for 5 min (Fig. 2). The product was purified by semipreparative high-performance liquid chromatography (HPLC) (μBondapak, C18 [Waters]; 7.8 × 300 mm; 10 μm; mobile phase, acetonitrile:0.1% phosphoric acid [30:70]; flow rate, 6 mL/min), and the retention time was 10−11 min. After removal of the HPLC solvent by rotary evaporation, the product was formulated using a 0.15 mol/L concentration of phosphate buffer, 10% EtOH, and 2% polysorbatum 80. ^{11}C-ABP688 was analyzed using analytic HPLC (BondClone, C18 [Phenomenex]; 3.9 × 300 mm; 5 μm; mobile phase, acetonitrile:0.1% phosphoric acid [30:70]; flow rate, 2 mL/min).

The position of the label was determined by repeating the synthetic procedure with ^{13}C-enriched methyl iodide under the same radiochemical reaction conditions.

Determination of Distribution Coefficient (Log D) and Plasma Stability

The lipophilicity of ^{11}C-ABP688 at pH 7.4 was determined as described by Strijckmans et al. (*20*). In vitro plasma stability was determined by incubating the radioligand in human plasma at 37°C for 60 min, and samples were analyzed by analytic HPLC.

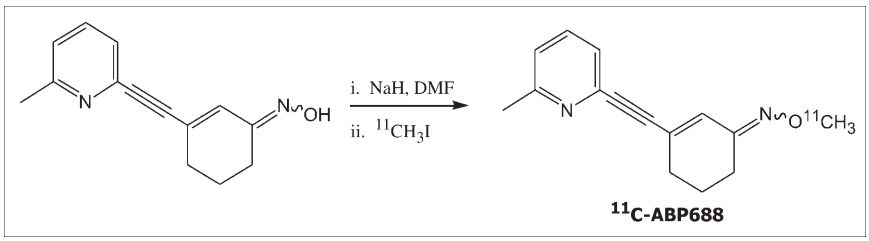

FIGURE 2. Radiosynthesis of ^{11}C-ABP688.

Animals

Animal care and all experimental procedures were approved by the Swiss Federal Veterinary Office. Animals (male Sprague–Dawley rats, 250−450 g, obtained from Charles River; female and male C57/BL6 wild-type (wt) and mGluR5-knock-out (ko) mice, 25−35 g, obtained from Novartis Pharma AG) were allowed free access to food and water.

In Vitro Binding of ^{11}C-ABP688

Preparation of Membranes. Male rats were euthanized by decapitation, and the brains were quickly removed individually. The whole brains without cerebellum were homogenized in 10 volumes of ice-cold (4°C) sucrose buffer (sucrose, 0.32 mol/L; Tris/acetate buffer, 10 mmol/L; pH 7.4) with a PT 1200 C Polytron (Kinematica AG) for 1 min at setting 4. The homogenate was centrifuged at 1,000*g* for 15 min (4°C) to yield a crude pellet (P1). This pellet was resuspended in 5 volumes of sucrose buffer, homogenized, and centrifuged again at 1,000*g* for 15 min (4°C). The resulting supernatants were combined and centrifuged at 17,000*g* for 20 min (4°C) to yield pellet P2. P2 was washed with ice-cold incubation buffer 1 (Tris/acetate buffer, 5 mmol/L; pH 7.4), homogenized, and centrifuged at 17,000*g* for 20 min (4°C). The P2 membrane pellet was resuspended in incubation buffer 1 and stored at −70°C. On the day of the assay, the P2 membranes were thawed and the protein concentration was determined by a Bio-Rad microassay with bovine serum albumin as a standard (*21*).

Saturation Experiments. A 500 μg/mL quantity of whole rat brain (without cerebellum) membranes were incubated with increasing concentrations of ^{11}C-ABP688 (0.5−100 nmol/L) in incubation buffer 2 (NaHEPES, 30 mmol/L; NaCl, 110 mmol/L; KCl, 5 mmol/L; $CaCl_2 \times H_2O$, 2.5 mmol/L; $MgCl_2$, 1.2 mmol/L; pH 8) to give a total volume of 200 μL. Nonspecific binding was determined in the presence of M-MPEP, 100 μmol/L. Incubations were allowed to proceed for 45 min at room temperature before being terminated by vacuum filtration over GF/C filters (Whatman) and thereafter presoaked for 1 h in incubation buffer 2 to reduce nonspecific binding. The membranes retained on the filters were rinsed twice with 4 mL of ice-cold incubation buffer 2. The radioactivity retained on the filters was determined using a γ-counter (Cobra II Auto-Gamma; Canberra Packard).

Data Analysis. Scatchard analysis was performed with the computer program Kell-Radlig (McPherson and Biosoft), and 3 independent experiments were performed.

Ex Vivo Autoradiography

^{11}C-ABP688 was injected into the tail vein of a rat (730 MBq, 4.0 nmol), a wt-mouse (110 MBq, 1.7 nmol), and a ko-mouse (202 MBq, 0.7 nmol). At 8 min after injection, the animals were sacrificed by decapitation. Brains were immediately removed and frozen in isopentane, which was cooled to −70°C. The frozen samples were cut into 20-μm horizontal sections using a cryostat and, without any washing, were placed on a phosphor imager screen for 2 h. The imaging plate data were analyzed by a BAS 800 II system (Fuji Film). The early time point of sacrifice (8 min after injection) was chosen because of the short physical half-life of the radiotracer and the time-consuming procedure to obtain and expose the brain slices.

Biodistribution Studies

Biodistribution studies were performed on rats and mice. A formulated solution of ^{11}C-ABP688 was administered into the tail vein of awake animals (rats: 50−450 MBq, 0.4−3.5 nmol; mice: 50−350 MBq, 0.5−2.5 nmol). Blockade studies were performed by coinjecting M-MPEP (1.0 mg/kg of body weight; 1:1 polyethylene glycol [2 mg/mL]:H_2O) with the radiotracer. The animals were sacrificed by decapitation (the rats 30 min and the mice 20 min after injection). Whole brains were rapidly removed individually and dissected into specific brain regions: hippocampus, striatum, cortex, and cerebellum. Blood, urine, and peripheral organs such as liver, kidney, muscle, and bone were also taken. Each brain region was weighed and tissue radioactivity was measured in a γ-counter (Cobra II Auto-Gamma). For all brain regions examined, the tissue distribution was determined using the percentage injected dose (normalized to the body weight of the animal) per gram of wet tissue (%ID norm/g organ).

PET Studies

PET of rats and mice was performed using a 16-module variant of the quad-HIDAC tomograph (Oxford Positron Systems) (*22*). Resolution at the center of the field of view was 1.0 mm. The animals (rats, wt-mice, and ko-mice) were anesthetized with isoflurane before injection of the radioligand. ^{11}C-ABP688 (18−22 MBq, 1−3 nmol) was administered by tail vein injection. The scan duration was 90 min for rats and 30 min for mice. PET data were acquired in list mode and reconstructed in user-defined time frames using the one-pass list-mode expectation maximization algorithm incorporating resolution recovery. The bin size was 0.3 mm, with a matrix size of $120 \times 120 \times 240$ for mouse and rat brain and $340 \times 340 \times 660$ for whole rat body. Image files were evaluated by region-of-interest analysis using the dedicated software PMOD (PMOD Technologies, Ltd.) (*23*). Time–activity curves were normalized to the injected dose per gram of body weight and expressed as standardized uptake values.

Metabolite Studies

^{11}C-ABP688 (350−600 MBq, 2.5−4 nmol) was administered into the tail vein of awake rats (n = 2, 250 and 400 g), and the animals were sacrificed by decapitation 30 min after injection. Brain, blood, and urine were taken and analyzed for radioactive metabolites. Analytic HPLC (BondClone, C18; 3.9 × 300; 5 μm; mobile phase, acetonitrile:0.1% phosphoric acid [65:35]; flow rate, 0.4 mL/min) was used for the analysis.

Brain. The rat brains were homogenized with phosphate buffer (pH 7.4; 1 mL). Acetonitrile (1.5 mL) was added, and the resulting homogenate was centrifuged (4,000 rpm, 5 min). The supernatant was analyzed by analytic HPLC using the conditions already mentioned.

Blood. Blood samples were centrifuged at 4,000 rpm for 5 min, and the plasma obtained was precipitated with perchloroacetic acid and again centrifuged. The supernatant was analyzed by analytic HPLC.

Urine. The whole sample was directly analyzed by analytic HPLC without further work-up.

RESULTS

Radiosynthesis of ^{11}C-ABP688

^{11}C-ABP688 was obtained in greater than 95% radiochemical purity, and the specific radioactivity ranged from 100 to 200 GBq/μmol. The total synthesis time was 45−50 min, and radiochemical yield was 35% ± 8% (n = 17). The identity of ^{11}C-ABP688 was confirmed by coinjection with a reference compound, which showed identical retention time under the same elution conditions. Stable ABP688 in the formulated solution amounted to 0.3−1.7 μg/mL.

^{13}C-NMR data of ABP688 showed an intensive signal at 61.5 ppm, which corresponded to the *O*-methyl-C-atom. Mass spectrometry showed molecular ion peaks at (MS [m/z] 242 [M^+ + 1]) and (MS [m/z] 243 [M^+ + 1]) for authentic and ^{13}C-enriched ABP688, respectively. The ^{13}C-NMR data unambiguously confirmed *O*-methylation and an *E/Z* isomeric ratio of at least 6:1. The assignment of the *E*- and *Z*-isomers was based on a rotating-frame Overhauser-effect spectroscopy cross peak between the oxime methyl group and the olefinic proton. And, as expected, the *Z*-isomer gave a lower chemical shift (123.1 ppm; *E*-isomer, 130.8 ppm) for the carbon bearing the olefinic proton. The most potent isomer (*E,* data not shown) could be consistently obtained as the major component of a more than 10:1 *E/Z* mixture by preheating the sodium salt of the precursor to 90°C and then adding ^{11}C-MeI at this temperature.

Determination of Distribution Coefficient (Log D) and Plasma Stability

The results from 3 independent determinations gave a log D value of 2.4 ± 0.1 for ^{11}C-ABP688. No degradation products were observed after the radioligand was incubated in human plasma at 37°C for 60 min.

In Vitro Binding of ^{11}C-ABP688

For the estimation of the dissociation constant (K_D) and the maximum number of binding sites (B_{max}), ^{11}C-ABP688 was used in saturation studies. The receptor binding of ^{11}C-ABP688 was found to be saturable (Fig. 3A). The Scatchard transformation of the saturation binding data gave a linear plot (Fig. 3B) suggesting a single high-affinity binding site with a K_D of 1.7 ± 0.2 nmol/L (n = 3) and a B_{max} of 231 ± 18 fmol/mg of protein.

Ex Vivo Autoradiography

Ex Vivo Autoradiography of Rat Brain. In rats, ex vivo autoradiography showed that the brain uptake of ^{11}C-ABP688 was highly selective, with high accumulation in known mGluR5-rich regions such as the hippocampus, caudate putamen, and cortex (Fig. 4A). Remarkably, individual hippocampal regions such as the dentate gyrus, the cornu ammonis-1 (CA1) region, and the stratum radiatum could be differentiated. In contrast, radioactivity accumulation in the cerebellum was negligible, confirming the low receptor expression in this region shown by immunohistochemistry (*25*).

Ex Vivo Autoradiography Using Wt- and mGluR5-Ko-Mice. In wt-mice (Fig. 4B), ex vivo autoradiography using ^{11}C-ABP688 showed a specific brain uptake, with a similar distribution pattern observed in the rat brain. The autoradiograms of mouse brain sections showed intense labeling of mGluR5-rich regions and negligible labeling in the cerebellum. In contrast, mGluR5-ko-mouse brain revealed a homogeneous and markedly reduced uptake throughout the brain (Fig. 4C).

Biodistribution Studies

Biodistribution Studies on Rats. Classic postmortem biodistribution studies were undertaken under both baseline and blockade conditions. The biodistribution data of ^{11}C-ABP688 in rats are shown in Figure 5. Relative high radioactivity accumulation was observed in mGluR5-rich brain regions such as the hippocampus, striatum, and cortex, whereas radioactivity uptake in the cerebellum was low. Radioactivity uptake ratios of 6.6 ± 0.1, 5.4 ± 0.1, and 4.6 ± 0.1 were obtained for the striatum, hippocampus, and cortex, respectively, using the cerebellum as a reference region. The specificity of ^{11}C-ABP688 binding was confirmed by blockade studies with M-MPEP, an antagonist for mGluR5 (*12*). Up to 80% specific binding was observed for the hippocampus and striatum. No blocking effects were observed in the cerebellum.

Of the peripheral organs examined (data not shown), the kidney and liver showed the highest radioactivity accumulations of 0.2 and 0.18 %ID norm/g of organ, respectively, under baseline conditions. The lung, blood, muscle, and bone showed a radioactivity uptake less than 0.1 %ID norm/g of organ. Under blocking conditions, the liver demonstrated an increased radioactivity uptake. No significant blocking effects were observed for other peripheral organs examined.

Biodistribution Studies on Wt- and mGluR5-Ko-Mice. Examination of the regional brain biodistribution of ^{11}C-ABP688 in wt-mice confirmed the distribution pattern observed in rats. The highest measured uptake of radioactivity was again in the hippocampus and striatum and the

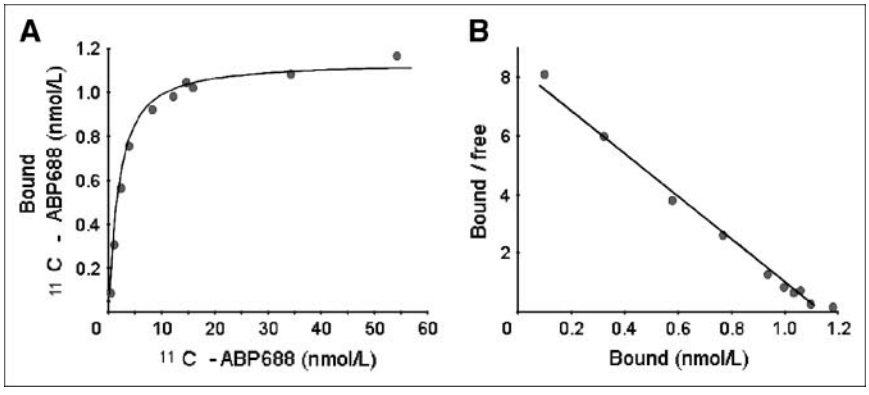

FIGURE 3. (A) Typical saturation curve of ^{11}C-ABP688 binding to rat brain membrane. (B) Representative Scatchard plot of ^{11}C-ABP688 binding. Results from 3 independent determinations gave a K_D of 1.7 ± 0.2 nmol/L and a B_{max} of 231 ± 18 fmol/mg of protein.

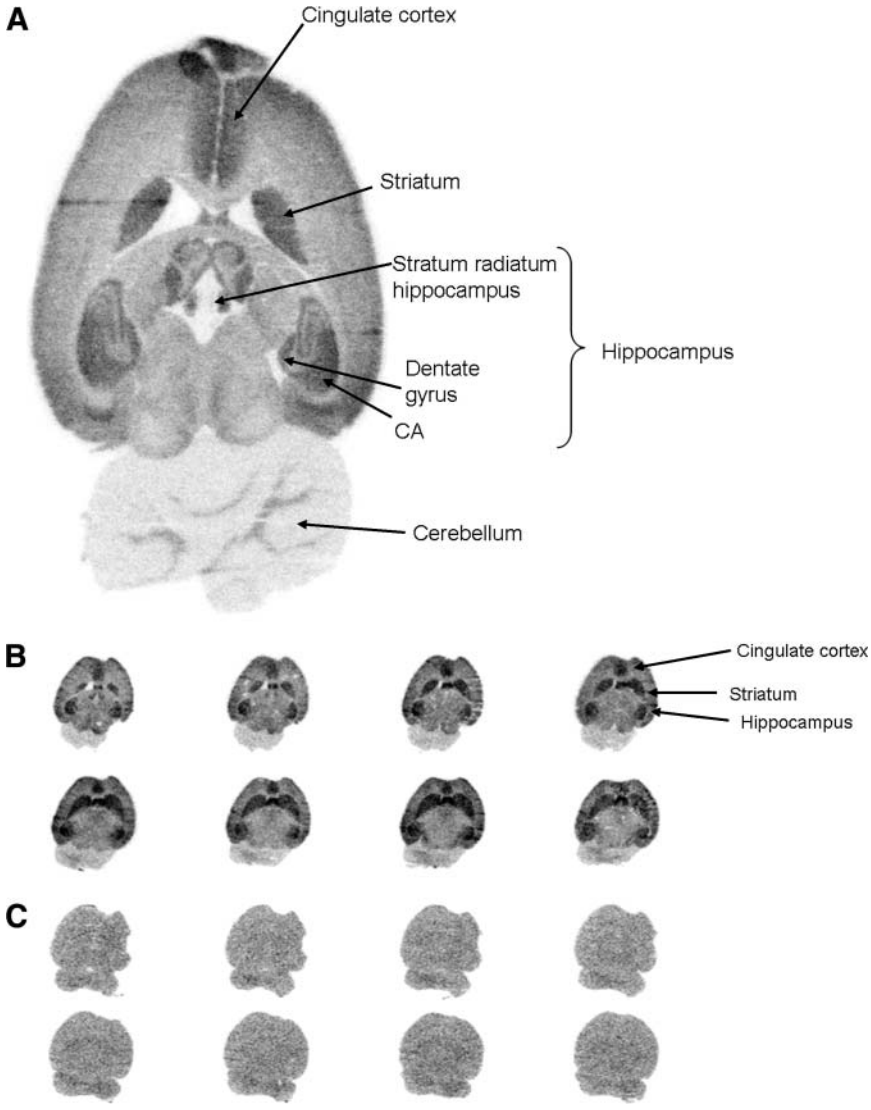

FIGURE 4. (A) Autoradiographic illustration of 20-μm unwashed horizontal (approximately −4.10 mm from Bregma and 5.90 mm interaural (*24*) slice of rat brain 8 min after intravenous injection of ^{11}C-ABP688. (B and C) Series of horizontal slices of ^{11}C-ABP688 distribution in wt-mouse (B) and ko-mouse (C).

lowest in the cerebellum. In contrast, radioactivity uptake was significantly less in mGluR5-ko-mice than in wt-mice and was identical in all the brain regions examined (Fig. 6). This finding nicely confirmed the extremely high in vivo selectivity observed in the blocking study on rats using mGluR5 antagonist M-MPEP.

PET Studies

Brain PET Studies on a Rat. A PET study performed on an anesthetized rat showed specific uptake of the radiotracer in mGluR5-rich brain regions such as the caudate putamen and hippocampus (Figs. 7A and 7B). ^{11}C-ABP688 binding in the brain was inhibited by coinjection of M-MPEP (1 mg/kg, intravenously) (Figs. 7C and 7D).

PET Studies on Wt- and mGluR5-Ko-Mice. As expected from ex vivo autoradiography, wt-mouse brain showed a heterogeneous uptake, with the highest uptake in the striatum and hippocampus. In contrast, mGluR5-ko-mice exhibited a homogeneous accumulation throughout the brain. A high radioactivity uptake was observed in extracerebral regions (i.e., nasal and lachrymal glands) both in the wt-mice and in the mGluR5-ko-mice (data not shown). These areas are known to nonspecifically accumulate central nervous system PET ligands (*25*). In wt-mice, a more than 2-fold radioactivity uptake was observed in the hippocampus, compared with the cerebellum. A similar ratio was obtained for the striatum. In contrast, the standardized uptake values in the whole forebrain and cerebellum of mGluR5-ko-mice were similar, suggesting only nonspecific uptake. These results indicate that the cerebellum could be used as a reference region for nonspecific uptake in future studies.

Metabolite Studies

HPLC analysis of whole-brain extracts from rats indicated that more than 95% of radioactivity in rat brain 30 min after radiotracer injection was parent compound (data not shown). Blood and urine samples were also analyzed by

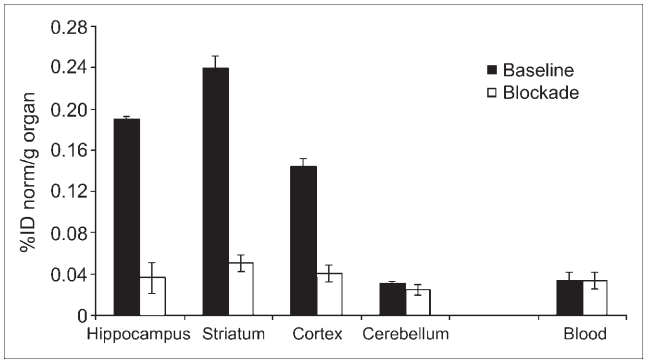

FIGURE 5. ^{11}C-ABP688 uptake in some brain regions of rat and in blood. Animals were sacrificed 30 min after injection. Control group (n = 3) received polyethylene glycol:H_2O (1:1) and ^{11}C-ABP688, and test group (n = 3) received coinjection of M-MPEP (1.0 mg/kg of body weight) and ^{11}C-ABP688. Data are expressed as percentage normalized injected dose (%ID norm) per gram of tissue ± SD.

HPLC, and most of the radioactivity (75% and 95%, respectively) could be attributed to radiolabeled metabolites, which were more polar than the parent compound. The extraction method used in this study proved suitable, because the recovery of radioactivity was greater than 90% in both brain and blood.

Taken together, these data suggest that ^{11}C-ABP688 has a favorable metabolic profile, including a rapid peripheral metabolism and no brain-penetrable metabolites.

DISCUSSION

Currently, no clinically validated PET tracer exists for mGluR5. In a recent publication, Hamill et al. (*17*) described 3 potential PET ligands and their characterization in rhesus monkeys. In this study, all 3 candidates exhibited selective uptake in the frontal cortex, striatum, and, surprisingly, the cerebellum, a brain region that has been shown to have a low or no expression of mGluR5 in rodents and humans (*26,27*). Yu et al. (*28*) also recently reported their evaluation of ^{11}C-MPEP and 2 of its derivatives in rats. The

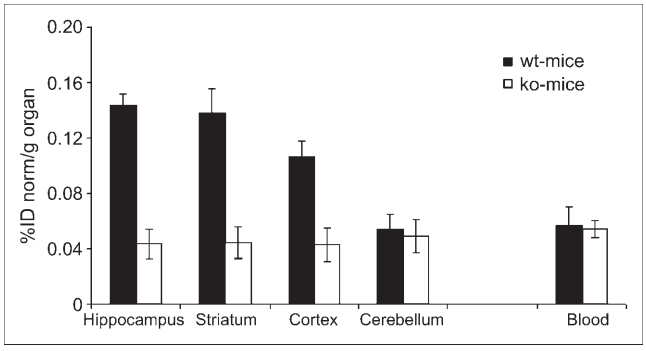

FIGURE 6. Biodistribution of ^{11}C-ABP688 in some brain regions of wt-mice (n = 4), mGluR5-ko-mice (n = 4), and blood. Animals were sacrificed 20 min after injection, and data are expressed as percentage of normalized injected dose (%ID norm) per gram of tissue ± SD.

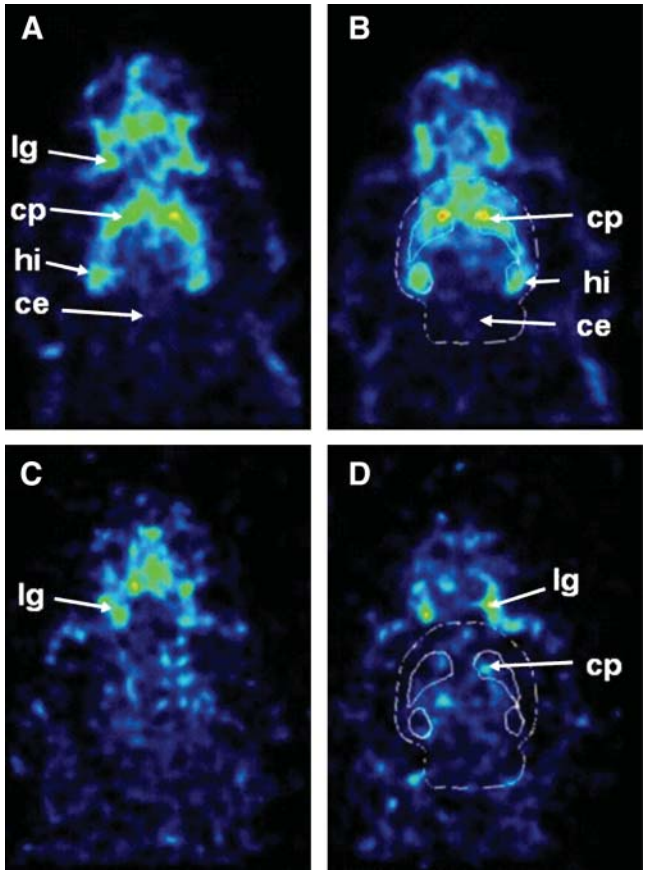

FIGURE 7. Representative horizontal images of ^{11}C-ABP688 uptake in head of 2 rats. Control animal (A and B) received 29.4 MBq (injected mass, 1.3 nmol) of radiotracer, and test animal (C and D) received coinjection of M-MPEP (1.0 mg/kg of body weight) and ^{11}C-ABP688 (5.37 MBq, injected mass, 1.7 nmol). Images were normalized to injected radioactivity and body weight. Data were reconstructed with bin size of 0.3 mm from 0 to 30 min after injection. ce = cerebellum; cp = caudate putamen; hi = hippocampus; lg = lacrimal gland. In B and D, whole brain and specific regions are bordered with white (*24*).

chemical modification of the original MPEP series allowed the identification of ABP688, a derivative in which the aromatic ring of the MPEP series is replaced by a functionalized cyclohexanone moiety (Fig. 1).

ABP688 was radiolabeled with ^{11}C in a simple 1-step procedure by *O*-methylation of the sodium salt of desmethyl-ABP688 using ^{11}C-methyl iodide. Purification by reversed-phase HPLC gave the final product in good radiochemical yields (35% ± 8%, n = 17) and high specific radioactivities (150 ± 50 GBq/μmol, n = 17) at the end of synthesis. A possible competing reaction is *N*-methylation of the pyridine nitrogen. Therefore, ^{13}C-ABP688 that had been synthesized and purified according to the procedure for the ^{11}C-labeled compound was characterized by ^{13}C-NMR and MS. The ^{13}C-NMR data of ABP688 obtained from the reaction of ^{13}C-CH_3I and desmethyl-ABP688 confirmed *O*-methylation. The lipophilicity of the tracer was determined experimentally using the shake-flask method. The measured log D value of 2.4 suggests that ^{11}C-ABP688 is

sufficiently lipophilic for free diffusion through the blood–brain barrier. For central nervous system PET ligands, a postulated log D value between 2 and 3 has been given as an optimal range for good blood–brain barrier penetration (*29*).

Saturation binding experiments using rat brain homogenates revealed a high B_{max} value of 231 ± 18 fmol/mg and a K_D of 1.7 ± 0.2 nmol/L, resulting in a favorable B_{max}/K_D ratio for a PET tracer (*21*). In rats and wt-mice, ex vivo autoradiography revealed a heterogeneous distribution pattern consistent with the known distribution of mGluR5 in the brain (*26,27,30*). The highest uptake was found in the hippocampus, striatum, and cortex. The cerebellum, a region with negligible mGluR5 density, showed the lowest brain uptake. The ultra high resolution of the method allowed differentiating between regions such as dentate gyrus, the CA1 region, and the stratum radiatum within the hippocampus (Fig. 4A).

Initial biodistribution studies in mice revealed a heterogeneous uptake of the tracer in the brain; the highest accumulation was observed in known mGluR5-rich regions such as striatum, hippocampus, and cortex, and a low uptake was observed in the cerebellum. The specificity of ^{11}C-ABP688 binding could be demonstrated with the help of mGluR5-ko-mice and using ex vivo autoradiography, which revealed homogeneous tracer uptake in all brain regions (*31*). The PET study also confirmed a markedly lower and more homogeneous brain uptake in mGluR5-ko-mice than in the wt-mice.

Postmortem biodistribution studies on rats also confirmed the heterogeneous radioactivity uptake in brain regions known to contain high densities of mGluR5. Radioactivity accumulation in the hippocampus and striatum was similar and amounted to 0.19 and 0.22 %ID norm/g of organ, respectively, at 30 min after injection. The observed heterogeneity of tracer uptake again corresponded to the reported distribution pattern of mGluR5. Blocking studies by coinjection of ^{11}C-ABP688 and unlabeled M-MPEP (1 mg/kg), a known selective mGluR5 antagonist, revealed up to 80% specific binding in mGluR5-rich rat brain regions (hippocampus, striatum, and cortex), whereas in the cerebellum, a region with negligible mGluR5 density, no significant changes in radioactivity uptake were observed (Fig. 5). A similar result was achieved in the PET study (Fig. 7), which showed specific uptake in the striatum and the hippocampus and low uptake in the cerebellum. The time–activity curves for striatum, hippocampus, and cerebellum reached a plateau shortly after tracer injection (data not shown) and remained constant during the entire PET scan. The specific tracer uptake in striatum and hippocampus could be inhibited by coinjection of the selective mGluR5 antagonist M-MPEP (1 mg/kg, intravenously). Taken together, these results confirmed the high selectivity of ^{11}C-ABP688 for mGluR5 in vivo.

Because radiolabeled metabolites may enter brain tissue and confound PET studies, we needed to verify that radioactive metabolites did not cross the blood–brain barrier; therefore, we directly examined rat brain extracts. The results indicated that more than 95% of the radioactivity found in the brain was parent compound 30 min after injection. The amount of radioactive metabolites—less than 5%—could be accounted for by the contribution from the brain vascular compartment. The extraction method proved suitable, because the recovery of radioactivity was greater than 90% in both brain and blood. Radiolabeled metabolites detected by HPLC were more hydrophilic than was the parent compound, suggesting that these metabolites would be too polar to enter the brain.

CONCLUSION

An efficient radiosynthesis for ^{11}C-ABP688, producing the tracer in good radiochemical yield and with high specific radioactivity, was developed. ^{11}C-ABP688 showed high affinity and specificity for mGluR5 in vitro and in vivo. Specific and heterogeneous brain uptake was confirmed by ex vivo autoradiography, postmortem biodistribution studies, and PET in rats. Biodistribution studies and PET in mGluR5-ko-mice confirmed the excellent specificity of the new ligand. Taken together, the preclinical profile of ^{11}C-ABP688 indicates that ^{11}C-ABP688 has the potential to become a valuable tracer for imaging mGluR5 distribution in humans using PET. Furthermore, it could be of great value for the selection of appropriate doses of clinically relevant candidate drugs that bind to mGluR5.

ACKNOWLEDGMENTS

We acknowledge the support of René Amstutz, the head of Discovery Technologies, and Graeme Bilbe, the head of neuroscience at the Novartis Institutes for Biomedical Research. We also thank Claudia Keller for technical assistance.

REFERENCES

1. Pin JP, Duvoisin R. The metabotropic glutamate receptors: structure and functions. *Neuropharmacology.* 1995;34:1–26.
2. Spooren WP, Gasparini F, Salt TE, Kuhn R. Novel allosteric antagonists shed light on mGluR5 and CNS disorders. *Trends Pharmacol Sci.* 2001;22:331–337.
3. Gereau RW, Conn PJ. Roles of specific metabotropic glutamate receptor subtypes in regulation of hippocampal CA1 pyramidal cell excitability. *J Neurophysiol.* 1995;74:122–129.
4. Spooren WP, Vassout A, Neijt HC, et al. Anxiolytic-like effects of the prototypical metabotropic glutamate receptor 5 antagonist 2-methyl-6-(phenylethynyl)pyridine in rodents. *J Pharmacol Exp Ther.* 2000;295:1267–1275.
5. Tatarczynska E, Klodzinska A, Chojnacka-Wojcik E, et al. Potential anxiolytic- and antidepressant-like effects of MPEP, a potent, selective and systemically active mGlu5 receptor antagonist. *Br J Pharmacol.* 2001;132:1423–1430.
6. Ohnuma T, Augood SJ, Arai H, McKenna PJ, Emson PC. Expression of the human excitatory amino acid transporter 2 and metabotropic glutamate receptors 3 and 5 in the prefrontal cortex from normal individuals and patients with schizophrenia. *Brain Res Mol Brain Res.* 1998;56:207–217.
7. Rouse ST, Marino MJ, Bradley SR, Awad H, Wittmann M, Conn PJ. Distribution and roles of metabotropic glutamate receptors in the basal ganglia motor circuit: implications for treatment of Parkinson's disease and related disorders. *Pharmacol Ther.* 2000;88:427–435.

8. Chiamulera C, Epping-Jordan MP, Zocchi A, et al. Reinforcing and locomotor stimulant effects of cocaine are absent in mGluR5 null mutant mice. *Nat Neurosci.* 2001;4:873–874.
9. Walker K, Bowes M, Panesar M, et al. Metabotropic glutamate receptor subtype 5 (mGluR5) and nociceptive function. I. Selective blockade of mGluR5 in models of acute, persistent and chronic pain. *Neuropharmacology.* 2001a; 40:1–9.
10. Walker K, Reeve A, Bowes M, et al. MGluR5 and nociceptive function II. MGluR5 functionally expressed on peripheral sensory neurones mediate inflammatory hyperalgesia. *Neuropharmacology.* 2001b;40:10–19.
11. Sotgiu ML, Bellomi P, Biella GE. The mGluR5 selective antagonist 6-methyl-2-(phenylethynyl)-pyridine reduces the spinal neuron pain-related activity in mononeuropathic rats. *Neurosci Lett.* 2003;342:85–88.
12. Gasparini F, Andres H, Flor PJ, et al. ^{3}H-M-MPEP, a potent subtype selective radioligand for the metabotropic glutamate receptor subtype 5. *Bioorg Med Chem Lett.* 2002;12:407–409.
13. Patel S, Krause SM, Hamill T, Chaudhary A, Burns HD, Gibson RE. In vitro characterization of ^{3}H-methoxypepy, an mGluR5 selective radioligand. *Life Sci.* 2003;73:371–379.
14. Gasparini F, Lingenhohl K, Stoehr N, et al. 2-Methyl-6-(phenylethynyl)-pyridine (MPEP), a potent, selective and systemically active mGluR5 antagonist. *Neuropharmacology.* 1999;38:1493–1503.
15. Ametamey SM, Kessler L, Honer M, Auberson Y, Gasparini F, Schubiger PA. Synthesis and evaluation of ^{11}C-FPEP as a PET ligand for imaging the metabotropic glutamate receptor subtype 5 (mGluR5) [abstract]. *J Labelled Compds Radiopharm.* 2003;46:188.
16. Kokic M, Honer M, Ametamey SM, et al. Radiolabeling and in vivo evaluation of ^{11}C-M-MPEP as a PET ligand for imaging the metabotropic glutamate receptor 5 (mGluR5) [abstract]. *J Labelled Compds Radiopharm.* 2001;44:231.
17. Hamill TG, Krause S, Ryan C, et al. Synthesis, characterization, and first successful monkey imaging studies of metabotropic glutamate receptor subtype 5 (mGluR5) PET radiotracers. *Synapse.* 2005;56:205–216.
18. Kessler LJ. *Development of Novel Ligands for PET Imaging of Metabotropic Glutamate Receptor Subtype 5 (mGluR5)* [dissertation no. 15633]. Zurich, Switzerland: Swiss Federal Institute of Technology Zurich; 2004. Available at: http://e-collection.ethbib.ethz.ch/show?type=diss&nr=15633). Accessed January 23, 2006.
19. Schönbächler R, Ametamey SM, Schubiger PA. Synthesis and ^{11}C-radiolabelling of a tropane derivative lacking the 2β-ester group: a potential tracer for the dopamine transporter. *J Labelled Compds Radiopharm.* 1999;42:447–456.
20. Strijckmans VH, Dolle F, Coulon C, et al. Synthesis of a potential M(1) muscarinic agent ^{76}Br-bromocaramiphen. *J Labelled Compds Radiopharm.* 1996;38:471–481.
21. Bradford MM. A rapid and sensitive method for the quantitation of microgram quantities of protein utilizing the principle of protein-dye binding. *Anal Biochem.* 1976;72:248–254.
22. Honer M, Bruhlmeier M, Missimer J, Schubiger PA, Ametamey SM. Dynamic imaging of striatal D2 receptors in mice using quad-HIDAC PET. *J Nucl Med.* 2004;45:464–470.
23. Mikolajczyk K, Szabatin M, Rudnicki P, Grodzki M, Burger CA. JAVA environment for medical image data analysis: initial application for brain PET quantitation. *Med Inform Lond.* 1998;23:207–214.
24. Paxinos G, Watson C. *The Rat Brain in Stereotaxic Coordinates.* New York, NY: Academic Press; 1998.
25. Myers R, Hume S, Bloomfield P, Jones T. Radio-imaging in small animals. *J Psychopharmacol.* 1999;13:352–357.
26. Daggett LP, Sacaan AI, Akong M, et al. Molecular cloning and characterization of recombinant human metabotropic glutamate receptor subtype 5. *Neuropharmacology.* 1995;34:871–886.
27. Romano C, Sesma MA, McDonald MT, O'Malley K, Van den Pol AN, Olney JW. Distribution of metabotropic glutamate receptor 5 (mGluR5) immunoreactivity in rat brain. *J Comp Neurol.* 1995;355:455–469.
28. Yu M, Tueckmantel W, Wang X, Zhu A, Kozikowski AP, Brownell AL. Methoxyphenylethynyl, methoxypyridylethynyl and phenylethynyl derivatives of pyridine: synthesis, radiolabeling and evaluation of new PET ligands for metabotropic glutamate subtype 5 receptors. *Nucl Med Biol.* 2005;32:631–640.
29. Wilson AA, Houle S. Radiosynthesis of carbon-11 labeled N-methyl 2-(arylthio)benzylamines: potential tracers for the serotonin reuptake receptor. *J Labelled Compds Radiopharm.* 1999;42:1277–1288.
30. Blumcke I, Behle K, Malitschek B, et al. Immunohistochemical distribution of metabotropic glutamate receptor subtypes mGluR1b, mGluR2/3, mGluR4a and mGluR5 in human hippocampus. *Brain Res.* 1996;736:217–226.
31. Eckelman WC. The use of gene-manipulated mice in the validation of receptor binding radiotracer. *Nucl Med Biol.* 2003;30:851–860.